

# *meso*-Octaethylporphyrinogen Displaying Site Selectivity in the Stepwise Synthesis of Polymetallic Aggregates with Interesting Redox Properties: The $\pi$ -Binding Ability of Metalla-Porphyrinogens

Lucia Bonomo,<sup>[a]</sup> Euro Solari,<sup>[a]</sup> Mario Latronico,<sup>[b]</sup> Rosario Scopelliti,<sup>[a]</sup> and Carlo Floriani\*<sup>[a]</sup>

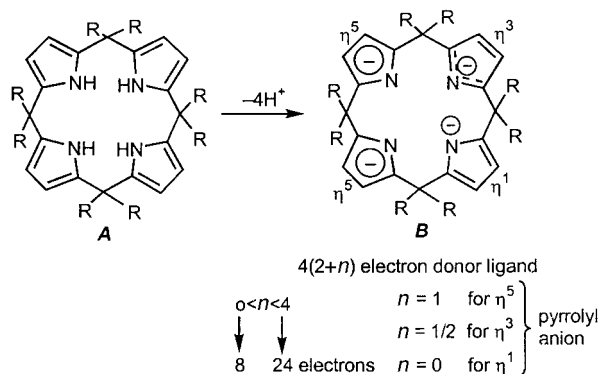
**Abstract:** The present report deals with the synthetic approach to homo- and heteronuclear polymetallic aggregates using the Ni<sup>II</sup>-*meso*-octaethylporphyrinogen complex  $[\{\eta^3-(\text{Et}_8\text{N}_4\text{Ni})\}\{\text{Li}(\text{thf})_2\}_2]$  (**1**) as a  $\pi$  ligand in the reaction with metal halides. The metallation reaction occurs via the probable intermediate of an isomeric form of **1**, namely **2**, which should be considered an organolithium derivative. Among the polymetallic aggregates, complexes  $[\{\eta^5-(\text{Et}_8\text{N}_4\text{Ni})\}_2\text{Co}] \cdot 2[\text{Li}(\text{thf})_4]$  (**6**) and  $[\{\eta^2-\eta^4-(\text{Et}_8\text{N}_4\text{Ni})\}_2\text{Ni}_2(\mu\text{-Cl})][\text{Li}(\text{thf})]$  (**8**) display a thermal and photochemical lability. Electron transfer reactions can be photochemically or thermally induced resulting in the formation of metal(0) and oxidized forms of the *meso*-octaethylporphyrinogen skeleton.

**Keywords:** coordination chemistry · porphyrinogens · tetrapyrroles · redox chemistry

## Introduction

The porphyrinogen skeleton, which has been considered in the past mainly for its redox relationship with porphyrin, in its stable form as *meso*-octaalkylporphyrinogen (**A**) has provided in recent years an unexpected and important entry to

organometallic and coordination chemistry.<sup>[1–3]</sup> Some of the major characteristics of the metal–porphyrinogen complexes are associated to the binding versatility of the porphyrinogen skeleton towards transition and non-transition metals.<sup>[4]</sup> The porphyrinogen tetraanion (**B**) allows, due to the conformation flexibility associated to the *meso*-sp<sup>3</sup> carbon atoms, each pyrrolyl anion to behave as an  $\eta^1$ ,  $\eta^3$ , or  $\eta^5$  binding site for a metal ion. This tetraanion can provide a variable number of electrons (from 8 up to 24) depending on the metal requirements along the reaction pathway.<sup>[5]</sup> Such a binding versatility of the porphyrinogen tetraanion has been observed in the complexation of early transition metals,<sup>[2]</sup> while in the case of late transition metals the electron-rich periphery functions as a binding site for alkali metal counterions.<sup>[3,4]</sup> We can consider, however, the porphyrinogen tetraanion (**B**) as displaying a site-binding selectivity providing a heteroatom environment, namely the N<sub>4</sub> core, and at the same time carbon ligands, namely the pyrrolyl anions, which can function as  $\eta^3$ - or  $\eta^5$ -binding sites.<sup>[1,2]</sup> This report focuses on establishing a strategy to use, in a sequential manner, the two different binding sites to build up polymetallic aggregates with interesting redox and magnetic properties. The synthetic strategy first requires to introduce a metal ion, which has a high preference for the N<sub>4</sub> site, followed by the exploitation of the  $\pi$ -binding ability of the pyrrolyl anions of the periphery.<sup>[5]</sup> This approach has been pursued binding nickel(II) first,<sup>[6]</sup> followed by its reaction with appropriate metal halides. The resulting polymetallic aggregates, which undergo electron transfer processes induced by ligand, heat, or light, led to



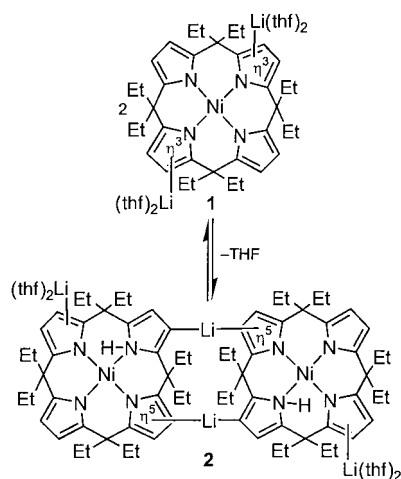
[a] Prof. Dr. C. Floriani, Dr. E. Solari, Dr. R. Scopelliti, L. Bonomo  
 Institut de Chimie Minérale et Analytique  
 Université de Lausanne  
 BCH 3307, CH-1015 Lausanne (Switzerland)  
 Fax: (+41)21-692-39-05  
 E-mail: carlo.floriani@icma.unil.ch

[b] Dr. M. Latronico  
 Dipartimento di Ingegneria e Fisica dell'Ambiente  
 Università della Basilicata  
 I-85100 Potenza (Italy)

oxidized forms of porphyrinogen, thus shedding light on the metal-assisted oxidations of the porphyrinogen skeleton.

## Results and Discussion

Complex **1**, which is the parent compound<sup>[6]</sup> used in this study for building up polymetallic aggregates, undergoes a quite interesting thermal rearrangement, leading to **2** (Scheme 1). Such a thermal rearrangement, which is a signal of the access



Scheme 1. The isomerization of the lithium–nickel–porphyrinogen complex.

to polymetallic systems, occurs in boiling toluene and leads to red crystals of **2** upon extraction with  $\text{Et}_2\text{O}$ . The desolvation of the lithium cation enhances its electrophilic properties and favors the attack at the  $\beta$ -position of a pyrrole ring of an adjacent porphyrinogen. This type of reaction has been widely explored in the case of organic electrophiles or in the deuteration reaction.<sup>[7]</sup> As in the reaction with organic

electrophiles, the electrophilic attack by the lithium cation is followed by the migration of a proton, which, in the present case, chooses nitrogen. The reversibility of the isomerization of **1** to **2**, which has been proved by dissolving **2** in THF, suggests that regardless of the solvent, the reactivity of **1** eventually occurs via the intermediacy of **2**. This aspect of the chemical behavior of **1** is particularly relevant to the reaction (vide infra) with transition metal halides which, in fact, undergo alkylation by an organolithium derivative. The nature of **2**, including its reversible transformation back to **1**, has been monitored by  $^1\text{H}$  NMR spectroscopy, in particular the hydrogen shift to the nitrogen of the pyrrole ring. The solid-state structure assigned by an X-ray analysis is in agreement with the proposed solution structure of **2** (Figure 1).

Crystallographic data and details associated with data collection are given in Table 1. Selected bond lengths and angles for complexes **2**, **3**, **5**, **6**, and **8** are listed in Table 2. Table 3 compares the most relevant conformational parameters for the five complexes.

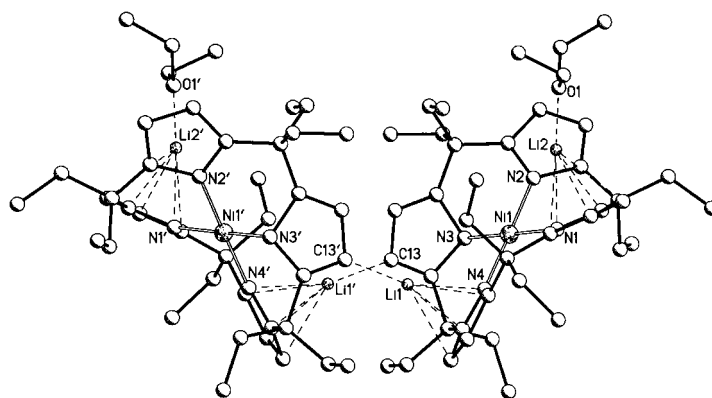


Figure 1. X-ray structure of complex **2**. Primes denote the symmetry transformation  $-x, y, 1/2 - z$ .

Table 1. Crystal data and structure refinement for **2**, **3**, **5**, **6**, and **8**.

	<b>2</b>	<b>3</b>	<b>5</b>	<b>6</b>	<b>8</b>
formula	$\text{C}_{80}\text{H}_{116}\text{Li}_4\text{N}_8\text{Ni}_2\text{O}_2$	$\text{C}_{46}\text{H}_{62}\text{N}_4\text{NiRu}$	$\text{C}_{44}\text{H}_{60}\text{N}_4\text{NiRu}$	$\text{C}_{72}\text{H}_{96}\text{CoN}_8\text{Ni}_2$ $\cdot 2\text{Li}(\text{C}_4\text{H}_{10}\text{O}_2)_3$ $\cdot 2\text{C}_6\text{H}_6$	$\text{C}_{72}\text{H}_{96}\text{CoN}_8\text{Ni}_4$ $\cdot \text{Li}(\text{C}_4\text{H}_{10}\text{O}_2)_3$ $\cdot 3/2(\text{C}_4\text{H}_{10}\text{O}_2) \cdot \text{C}_4\text{H}_8\text{O}_2$
Fw	1366.99	830.78	804.74	1960.73	1844.44
$T$ [K]	296	143	143	143	143
$\lambda$ [Å]	1.54178	1.54178	1.54178	0.71073	0.71070
crystal system	monoclinic	monoclinic	monoclinic	monoclinic	monoclinic
space group	$C2/c$	$P2_1/n$	$P2_1$	$P2_1/c$	$P2_1/c$
$a$ [Å]	33.895(8)	10.239(2)	9.378(4)	18.349(2)	19.380(6)
$b$ [Å]	11.356(6)	20.567(2)	11.897(2)	12.2681(10)	22.912(3)
$c$ [Å]	20.258(6)	19.314(2)	17.197(3)	23.590(3)	23.730(6)
$\alpha$ [°]	90	90	90	90	90
$\beta$ [°]	101.95(2)	90.19(3)	101.94(3)	95.314(9)	111.69(2)
$\gamma$ [°]	90	90	90	90	90
$V$ [Å <sup>3</sup> ]	7628(5)	4067.5(10)	1877.1(9)	5287.5(10)	9791(4)
$Z$	4	4	2	2	4
$\rho_{\text{calcd}}$ [g cm <sup>-3</sup> ]	1.190	1.357	1.424	1.232	1.251
$\mu$ [mm <sup>-1</sup> ]	0.986	3.848	4.150	0.569	0.844
reflections collected	6840	7357	3694	21007	57602
data/parameters	6720/434	7136/470	3469/232	8693/589	17039/1073
$RI$ [ $I > 2\sigma(I)$ ]	0.0743	0.0413	0.0584	0.0687	0.0696
$wR2$ (all data)	0.2859	0.1260	0.1600	0.2229	0.2279

Table 2. Selected bond lengths [Å] and angles [°] for complexes **2**, **3**, **5**, **6**, and **8**.<sup>[a]</sup>

<b>2</b>					
Ni1–N1	1.887(7)	Li1– $\eta^5$ (Pyr)	2.05(2)	Li2–O1	1.84(3)
Ni1–N2	1.902(7)	Li1–C13'	1.98(2)	C13'–Li1– $\eta^5$ (Pyr)	163(1)
Ni1–N3	2.039(9)	Li2– $\eta^5$ (Pyr)	2.13(2)	O1–Li2– $\eta^5$ (Pyr)	135(1)
Ni1–N4	1.914(8)	prime denotes the symmetry transformation: $-x, y, 1/2 - z$			
<b>3</b>					
Ni1–N1	1.921(4)	Ni1–N4	1.883(4)	Ru1– $\eta^6$ ( <i>p</i> -cymene)	1.745(5)
Ni1–N2	1.888(4)	Ru1– $\eta^5$ (Pyr)	1.846(5)	$\eta^5$ (Pyr)–Ru1– $\eta^6$ ( <i>p</i> -cymene)	176.6(2)
Ni1–N3	1.867(4)				
<b>5</b>					
Ni1–N1	1.90(1)	Ru1– $\eta^5$ (Pyr)	1.82(1)	C16–C17	1.55(2)
Ni1–N2	1.875(9)	Ru1– $\eta^5$ (C <sub>8</sub> H <sub>9</sub> )	1.81(1)	C17–C18	1.55(2)
Ni1–N3	1.88(1)	$\eta^5$ (Pyr)–Ru1– $\eta^5$ (C <sub>8</sub> H <sub>9</sub> )	178.5(5)	C18–C19	1.52(2)
Ni1–N4	1.91(1)	N4–C16	1.49(2)	N4–C19	1.29(2)
C <sub>8</sub> H <sub>9</sub> =trihydropentalene					
<b>6</b>					
Ni1–N1	1.895(4)	Ni1–N3	1.853(4)	Co1– $\eta^5$ (Pyr)	1.802(5)
Ni1–N2	1.855(4)	Ni1–N4	1.850(4)	$\eta^5$ (Pyr)–Co1– $\eta^5$ (Pyr)'	180
prime denotes the symmetry transformation: $-x, -y, -z$					
<b>8</b>					
Ni1–N1	1.912(3) [1.896(4)]	Ni3–C3	2.163(4)	Ni4–C44	2.145(5)
Ni1–N2	1.909(4) [1.905(4)]	Ni3–C4	2.373(4)	Ni4–C45	2.362(4)
Ni1–N3	1.872(4) [1.871(4)]	Ni3–C38	2.336(4)	Ni4–C7	2.118(4)
Ni1–N4	1.874(4) [1.867(4)]	Ni3–C39	2.114(4)	Ni4–C8	2.302(4)
Ni3– $\eta^4$ (Pyr)	1.936(4)	Ni4– $\eta^4$ (Pyr)	1.944(5)	Ni3–Cl1	2.241(1)
Ni3– $\eta^2$ (Pyr)	2.108(4)	Ni4– $\eta^2$ (Pyr)	2.089(4)	Ni4–Cl1	2.238(1)
Ni3–C1	2.337(4)	Ni4–C42	2.371(4)	Ni3–Cl1–Ni4	105.32(5)
Ni3–C2	2.132(5)	Ni4–C43	2.162(5)		
Values in square brackets refer to the second Ni <sup>II</sup> –porphyrinogen moiety: Ni2, N5, N6, N7, N8.					

[a]  $\eta^5$ (Pyr),  $\eta^4$ (Pyr),  $\eta^2$ (Pyr),  $\eta^6$ (*p*-cymene) indicate the centroids.

The two Ni<sup>II</sup>–porphyrinogen moieties are linked by two lithium atoms, each of them showing an  $\eta^5$ ,  $\eta^1$  coordination mode<sup>[4,5,6,8]</sup> across two Ni–porphyrinogen moieties (Li1– $\eta^5$ (N4–C16–C17–C18–C19) 2.05(2), Li1– $\eta^1$ (C13') 1.98(2), Li2– $\eta^5$ (N1–C1–C2–C3–C4) 2.13(2), Li2– $\eta^1$ (O1) 1.84(3) Å). The lithium atom Li1' is bonded to the  $\beta$ -carbon (C13) of the pyrrole containing the protonated nitrogen (N3). Ni1 lies out of the plane of the N<sub>4</sub> core and the protonated pyrrole plane by  $-0.026(4)$  Å and  $1.972(9)$  Å, respectively. The latter value shows the relative change in the orientation of the protonated versus the other pyrroles. The Ni–N bond

lengths (Ni1–N1 1.887(7), Ni1–N2 1.902(7), Ni1–N3 2.039(9), Ni1–N4 1.914(8)) show, once again, the presence of the proton on N3.

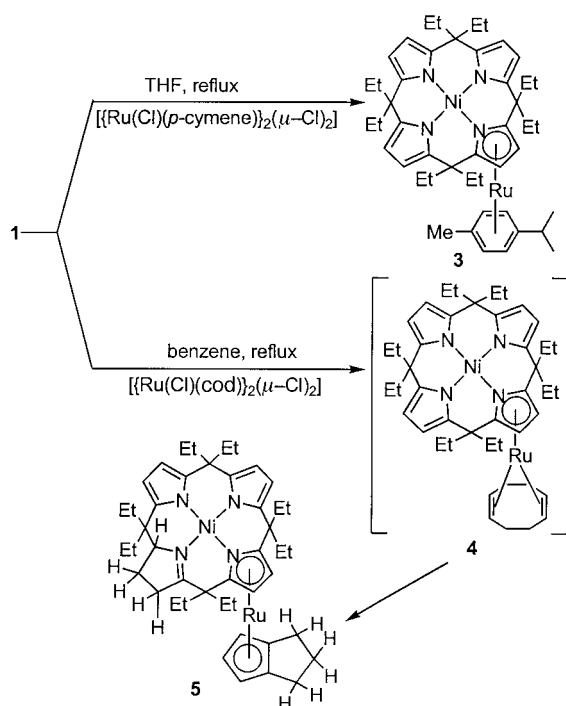
The  $\pi$ -binding ability of the periphery of the Ni–porphyrinogen complex **1** was preliminarily explored in the reaction with [RuCl<sub>2</sub>] fragments.<sup>[9]</sup> For this purpose we employed [[Ru(Cl)(*p*-cymene)]<sub>2</sub>( $\mu$ -Cl)<sub>2</sub>]<sup>[10]</sup> and [[Ru(Cl)(cod)]<sub>2</sub>( $\mu$ -Cl)<sub>2</sub>]<sup>[11]</sup> (cod = 1,2-cyclooctadiene), in which the coordination sphere of the metal is partially filled by the aromatic ring or the diolefin, respectively. The metalation of **1** by the aforementioned ruthenium derivatives, carried out

Table 3. Comparison of relevant structural parameters within the metal–porphyrinogen units for complexes **2**, **3**, **5**, **6**, and **8**.

	<b>2</b>	<b>3</b>	<b>5</b>	<b>6</b>	<b>8</b>	
distance of atoms from the N <sub>4</sub> core [Å]	N1	0.068(4)	-0.053(2)	0.018(5)	-0.044(2)	0.007(2)
	N2	-0.068(4)	0.053(2)	-0.018(5)	0.044(2)	-0.007(2)
	N3	0.062(4)	-0.053(2)	0.018(5)	-0.044(2)	0.007(2)
	N4	-0.062(4)	0.054(2)	-0.017(5)	0.044(2)	-0.007(2)
	Ni1	-0.026(4)	-0.031(2)	-0.022(6)	-0.025(2)	0.003(2)
distance of Ni1 from A <sup>[a]</sup> [Å]		-0.40(2)	0.274(7)	0.20(2)	0.345(7)	-0.013(7)
distance of Ni1 from B <sup>[a]</sup> [Å]		-0.06(1)	0.083(8)	-0.34(2)	-0.215(8)	0.392(6)
distance of Ni1 from C <sup>[a]</sup> [Å]		1.972(9)	0.131(8)	0.51(2)	-0.062(8)	-0.196(7)
distance of Ni1 from D <sup>[a]</sup> [Å]		0.01(1)	-0.296(8)	0.14(2)	-0.217(9)	-0.079(8)
angles between the N <sub>4</sub> core and the A, B, C, D rings [°]	(A)	37.6(4)	34.7(2)	30.5(5)	36.1(2)	31.0(2)
	(B)	37.6(4)	27.0(2)	36.1(5)	37.0(2)	35.7(2)
	(C)	75.3(3)	30.0(2)	39.9(5)	31.9(2)	29.8(2)
	(D)	28.2(5)	34.6(2)	24.5(5)	30.9(2)	28.4(2)
angle between AB [°]		58.2(4)	51.5(2)	47.0(6)	46.4(2)	54.0(2)
angle between BC [°]		40.2(4)	38.2(2)	56.6(5)	41.4(2)	42.1(2)
angle between CD [°]		77.7(3)	36.3(2)	33.0(7)	38.3(2)	33.3(2)
angle between AD [°]		38.9(5)	46.4(2)	44.3(5)	57.8(3)	42.6(3)

[a] A, B, C and D define the pyrrole rings containing N1, N2, N3 and N4. [b] The double values for **8** refer to the two different Ni<sup>II</sup>–porphyrinogen units

either in boiling THF or in benzene, led to complexes **3** and **5** (Scheme 2), which were recovered in high yield as crystalline solids. Under such thermal conditions we suppose that the desolvated form **2** may be the active intermediate in the



Scheme 2. The  $\pi$  complexation of ruthenium(II) by nickel-porphyrinogen.

transmetalation reaction. In complex **3**, one of the pyrrolyl anions, which is  $\eta^1$ -N bonded to Ni<sup>II</sup>, acts as an  $\eta^5$ -cyclopentadienyl-like ligand towards Ru<sup>II</sup>.<sup>[12]</sup> The reaction leads to **3** regardless of the Ni/Ru stoichiometric ratio. The reaction of **1** with  $[[\text{Ru}(\text{Cl})(\text{cod})]_2(\mu\text{-Cl})_2]$  proceeds, at least in a preliminary stage, quite similarly to that with  $[[\text{Ru}(\text{Cl})(p\text{-cymene})]_2(\mu\text{-Cl})_2]$ .

The formation of the proposed intermediate **4** is followed, however, by the Ru-assisted isomerization of the cod ligand to the trihydropentalene monoanion and the hydrogen transfer to one of the pyrrole rings of the Ni-porphyrinogen fragment (see complex **5** in Scheme 2). The Ru-assisted hydrogen transfer reaction is not particularly unusual,<sup>[13,14]</sup> while the formation of pentalene skeleton<sup>[14]</sup> from cod and the hydrogen transfer to a macrocyclic structure is interesting in the context of the unique properties associated with polymetallic systems.

The characterization of **3** and **5** has been carried out both in solution by <sup>1</sup>H NMR spectroscopy (see Experimental Section) and in the solid state by X-ray analysis. In complex **3** (Figure 2, Table 2) the Ni<sup>II</sup>-porphyrinogen moiety shows the usual saddle-shape conformation (Table 3) and, as expected, Ni1 is only slightly out of the plane of the N<sub>4</sub> moiety ( $-0.031(2)$  Å). The Ni1–N bond lengths vary in a narrow range from 1.867(4) to 1.921(4) Å; the longest one is Ni1–N1, which is associated to the pyrrole  $\eta^5$ -bonded [N1,C1,C2,C3,C4] to ruthenium.<sup>[9,12,16]</sup> The Ru–pyrrole and Ru–arene<sup>[9,12,15]</sup> distances are in the usual range (Ru1– $\eta^5$  1.846(5), Ru1– $\eta^6$  1.745(5) Å).

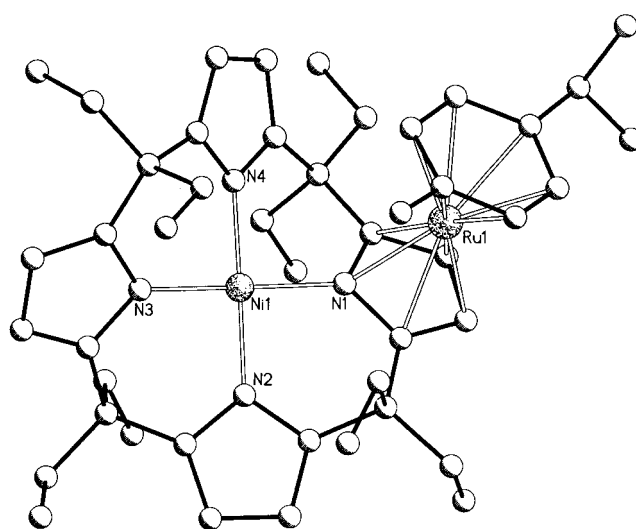


Figure 2. X-ray structure of complex **3**.

In complex **5** (Figure 3), the structural parameters concerning the Ni<sup>II</sup>-porphyrinogen moiety are in the range observed for the other Ni-porphyrinogen derivatives: Ni1 is out of the plane of the N<sub>4</sub> inner core by  $-0.022(6)$  Å; the Ni1–N bond lengths (Ni1–N1 1.90(1), Ni1–N2 1.875(9), Ni1–N3 1.88(1), Ni1–N4 1.91(1)) show only slightly the effects due to the  $\eta^5$  bonding mode to Ru<sup>II</sup>. The peculiar aspect of this structure is

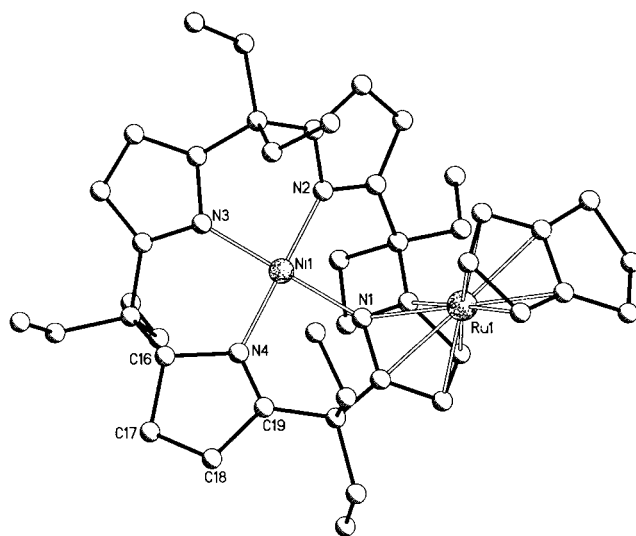
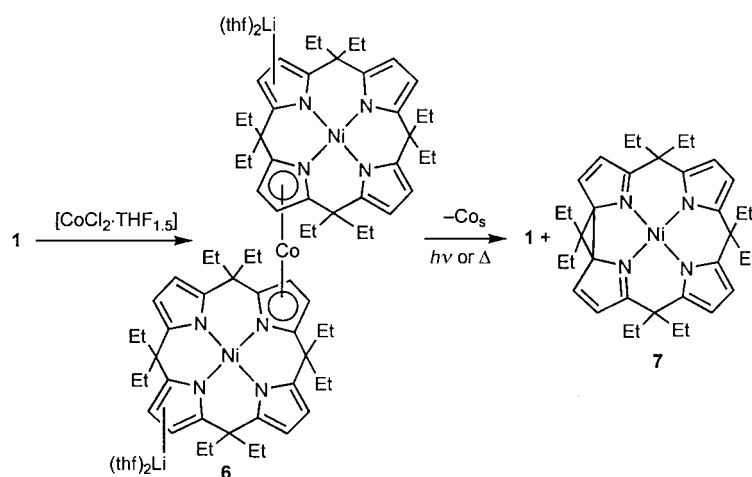


Figure 3. X-ray structure of complex **5**.

the rearrangement of the cod ligand into the trihydropentalene monoanion, which occurs with the transfer of the three hydrogen atoms to one of the pyrrole rings (N4–C16–C17–C18–C19), C16 having an *R* absolute configuration. Ruthenium(II) is  $\eta^5$ -bonded (1.81(1) Å) to the trihydropentalene monoanion and  $\eta^5$ -bonded (1.82(1) Å)<sup>[14]</sup> to one of the pyrrolyl moieties (N1,C1,C2,C3,C4).<sup>[9,12,16]</sup>

When complex **1** was metalated with metal halides that do not contain any protecting organic fragment, two classes of compounds were identified depending on the stoichiometric ratio (see Schemes 3 and 4). The reaction of **1** with  $[\text{CoCl}_2 \cdot$



Scheme 3. The nickel–porphyrinogen sandwiching cobalt in a cobaltocene-type structure and its photochemical decomposition.

THF<sub>1.5</sub>] in a 2:1 molar ratio led to the formation of the paramagnetic ( $\mu_{\text{eff}} = 1.80 \mu_{\text{B}}$  at 293 K) cobaltocene-type derivative **6** (Scheme 3). The structure of the dianion form **6** is shown in Figure 4, and the structural parameters are given in Table 2. The Ni<sup>II</sup> ion is coplanar with the N<sub>4</sub> core of the

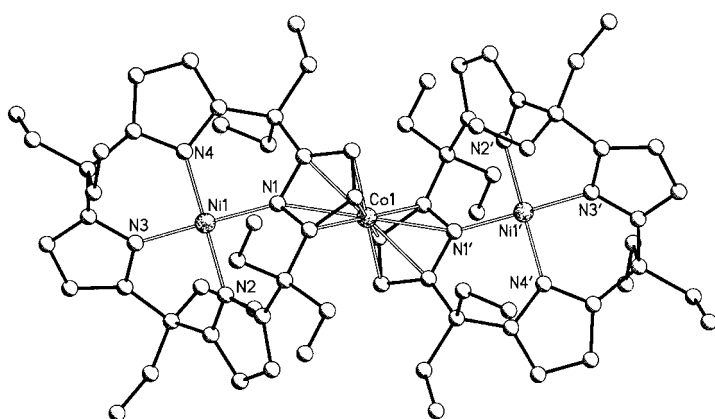


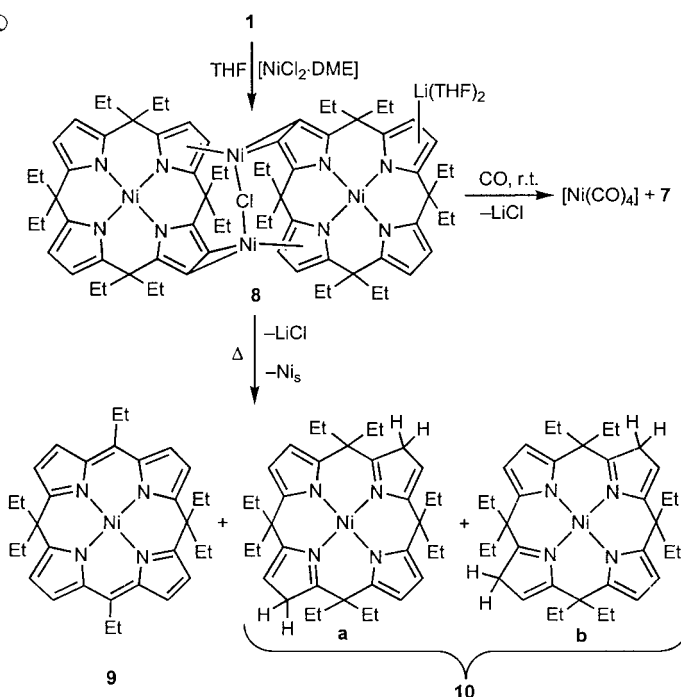
Figure 4. X-ray structure of the anion in complex **6**, the counterion is [Li(dme)<sub>3</sub>]<sup>+</sup>. Primes denote the symmetry transformation  $-x, -y, -z$ .

porphyrinogen, which has a distorted saddle-shaped conformation.<sup>[6]</sup> The longer Ni–N distance (Ni1–N1 1.895(4) Å) is related to the pyrrole binding the cobalt in the  $\eta^5$ -bonding fashion (Co–(Pyr)<sub>centroid</sub> 1.802(5) Å; (Pyr)<sub>centroid</sub>–Co–(Pyr)<sub>centroid</sub> 180°, from symmetry requirements). The structural parameters related to the cobalt environment should be compared with those of some cobaltocene analogues.<sup>[17]</sup> The  $\eta^5$ -bonding mode is assumed, though a significant variation in the Co–C and Co–N distances has been observed (Co1–C1 2.184(5), Co1–C2 2.059(5), Co1–C3 2.051(5), Co1–C4 2.190(5), Co1–N1 2.305(4) Å). One of the most attractive characteristics of such polymetallic aggregates is associated with their redox properties. Complex **6** undergoes a photochemically or thermally induced intramolecular redox reaction (Scheme 3). In the former case, irradiation of **6** using visible light led to the separation of cobalt metal and the two-electron oxidized form of the Ni–porphyrinogen containing a cyclopropane func-

tionality (**7**)<sup>[3]</sup> along with **1**. In the case of the thermal decomposition, the products derived from the thermally induced transformations of **7** were identified, instead of **7** itself.<sup>[18]</sup> The overall photochemical reaction, corresponding to the one-electron oxidation of the Ni–porphyrinogen complex, led to an equimolar amount of the two-electron oxidized species **7** and the starting complex **1**. The thermally and photochemically induced electron transfer in polymetallic species is a relevant property, which we can take advantage of to design metastable redox couples.<sup>[19]</sup> In

addition, the formation of transient polymetallic systems should be considered as a valuable approach to the practical study of electron transfer processes. In particular, the oxidation of *meso*-octaalkylporphyrinogens to the so-called artificial porphyrins<sup>[1b,3]</sup> by using CuCl<sub>2</sub> can be viewed as occurring by the preliminary formation of a dimetallic porphyrinogen complex.

Complex **1** undergoes a different kind of metalation using [NiCl<sub>2</sub>·DME<sub>1.5</sub>] (1:1 molar ratio) in THF. The reaction led to the formation of the tetranickel derivative **8** (Scheme 4), which contains two diamagnetic square-planar and two paramagnetic Ni<sup>II</sup> ions (2.85  $\mu_{\text{B}}$  at 295 K *per* nickel). The structure of **8** (Figure 5) has been elucidated by X-ray analysis. The two Ni<sup>II</sup>–porphyrinogen moieties are bridged by two Ni<sup>II</sup> ions



Scheme 4. A tetranuclear nickel–porphyrinogen complex undergoing thermal and CO-induced demetalation.

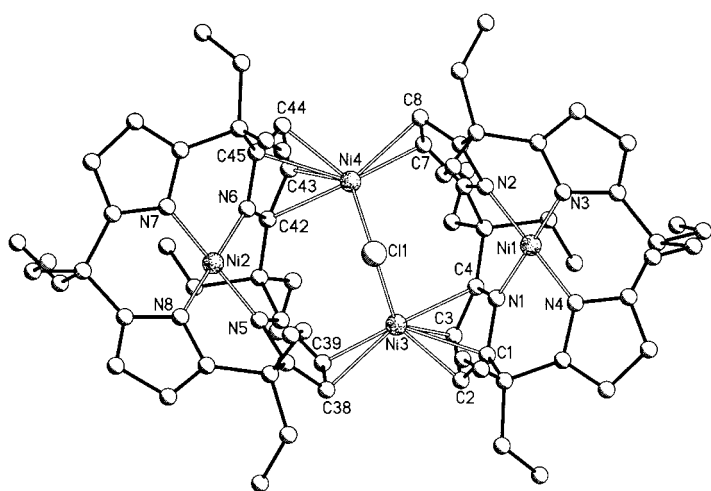


Figure 5. X-ray structure of the anion in complex **8**, the counteranion is  $[\text{Li}(\text{dme})_3]^+$ .

connected by a single Cl ion ( $\text{Ni}-\text{Cl}_{\text{av}}$  2.239(1) Å). The longer Ni–N bond lengths within the two Ni–porphyrinogen units are related to the pyrroles shared with the two peripheral nickel ions ( $\text{Ni}-\text{N}_{\text{av}}$  1.906(4) vs  $\text{Ni}-\text{N}_{\text{av}}$  1.871(4) Å). The binding of the  $[\text{Ni}_2\text{Cl}]$  fragment induces considerable distortions on the Ni–porphyrinogen moieties, though Ni1 and Ni2 remain coplanar with the  $\text{N}_4$  set of donor atoms. The bonding mode of the bridging nickel ions approximates that of an  $\eta^4$ -diene ( $\text{Ni}3-(\text{C}1, \text{C}2, \text{C}3, \text{C}4)_{\text{centroid}}$  1.936(4),  $\text{Ni}4-(\text{C}42, \text{C}43, \text{C}44, \text{C}45)_{\text{centroid}}$  1.944(5) Å) and an  $\eta^2$ -olefin ( $\text{Ni}3-(\text{C}38, \text{C}39)_{\text{centroid}}$  2.108(4),  $\text{Ni}4-(\text{C}7, \text{C}8)_{\text{centroid}}$  2.089(4) Å). These values are similar to some Ni–diene and Ni–olefin bond lengths reported.<sup>[20]</sup> The pseudo-tetrahedral coordination spheres around Ni3 and Ni4 are in agreement with their high-spin state.

Complex **8** undergoes an oxidative demetalation using carbon monoxide with the formation of **7** and  $[\text{Ni}(\text{CO})_4]$ . The very high stabilization of Ni(0) by carbon monoxide forces the Ni–porphyrinogen to function as an oxidizing agent releasing two electrons. The two-electron oxidation of Ni–porphyrinogen **1**, that is using *p*-benzoquinone, led to the formation of the corresponding monocyclopropane derivative **7**,<sup>[1b,3]</sup> as is the case in the reaction of **8** with carbon monoxide. The thermally induced demetalation of **8** proceeds with the formation of a nickel mirror and an equimolar mixture of **9**<sup>[18]</sup> and the two isomers of **10**<sup>[7]</sup> (Scheme 4). Although the thermal reaction seems very different from the photochemical one in Scheme 3 and the CO-induced demetalation, a close relationship between them can be found.<sup>[18]</sup> In the formation of the porphodimethene–nickel complex **9**,<sup>[18]</sup> a four-electron oxidation of the porphyrinogen skeleton is coupled with the formation of the two isomers **10a** and **10b**.<sup>[7]</sup>

## Experimental Section

**General Procedure:** All reactions were carried out under an atmosphere of purified nitrogen. Solvents were dried and distilled before use by standard methods. <sup>1</sup>H NMR and IR spectra were recorded on AC-200, DPX-400 Bruker, and Perkin–Elmer FT 1600 instruments, respectively. GC and GC-MS analyses were carried out using a HP 5890 Series II system and a HP

5890A GC system, respectively. Magnetic susceptibility measurements were made on an Quantum Design MPMS5 SQUID susceptometer operating at a magnetic field strength of 1 kOe. The syntheses of  $[\{\text{Ru}(\text{Cl})(p\text{-cymene})_2(\mu\text{-Cl})_2\}]^{[10]}$ ,  $[\{\text{Ru}(\text{Cl})(\text{cod})_2(\mu\text{-Cl})_2\}]^{[11]}$  and **1**<sup>[6,5]</sup> have been carried out as previously reported.

**Synthesis of 2:** A solution of **1** (30.0 g, 33.4 mmol) in toluene (300 mL) was refluxed overnight. The solution was evaporated to dryness and the solid residue was extracted with  $\text{Et}_2\text{O}$  (200 mL) to give a microcrystalline pink-red residue which was collected and dried in vacuo (16.2 g, 71%). Crystals suitable for X-ray diffraction were grown in  $\text{Et}_2\text{O}$ . <sup>1</sup>H NMR ( $\text{C}_6\text{D}_6$ , 200 MHz, 298 K):  $\delta$  = 7.52 (s, 2H; NH), 6.27 (d,  $J$  = 2.4 Hz, 2H;  $\text{C}_4\text{H}_2\text{N}$ ), 6.12 (s br., 4H;  $\text{C}_4\text{H}_2\text{N}$ ), 5.89 (m, 6H;  $\text{C}_4\text{H}_2\text{N}$ ), 5.81 (d,  $J$  = 2.9 Hz, 2H;  $\text{C}_4\text{H}_2\text{N}$ ), 5.00 (m, 2H;  $\text{CH}_2$ ), 4.84 (m, 2H;  $\text{CH}_2$ ), 4.60 (m, 2H;  $\text{CH}_2$ ), 4.28 (m, 2H;  $\text{CH}_2$ ), 3.25 (m, 2H;  $\text{CH}_2$  overlapping with q,  $J$  = 7.3 Hz, 8H;  $\text{Et}_2\text{O}$ ), 2.83 (m, 2H;  $\text{CH}_2$ ), 2.48 (m, 2H;  $\text{CH}_2$ ), 2.3–1.3 (m, 18H;  $\text{CH}_2$ ), 1.13 (t,  $J$  = 7.3 Hz, 12H;  $\text{Et}_2\text{O}$ ), 1.1–0.8 (m, 48H;  $\text{CH}_3$ ); **2**:  $\text{C}_{80}\text{H}_{116}\text{Li}_4\text{N}_8\text{Ni}_2\text{O}_2$ ; calcd C 70.29, H 8.55, N 8.20; found C 69.93, H 8.92, N 7.97.

**Synthesis of 3:**  $[\{\text{Ru}(\text{Cl})(p\text{-cymene})_2(\mu\text{-Cl})_2\}]$  (1.49 g, 2.44 mmol) was refluxed with **1** (4.38 g, 4.88 mmol) in THF (100 mL) for 12 h. The solvent was evaporated and benzene (100 mL) was added. The undissolved LiCl was filtered off and the resulting solution was evaporated to dryness. The solid residue was triturated with *n*-hexane to give a red powder, which was collected and dried in vacuo (3.47 g, 85%). Crystals suitable for X-ray diffraction were grown in a mixture of THF/*n*-hexane. <sup>1</sup>H NMR ( $\text{C}_5\text{D}_5\text{N}$ , 200 MHz, 298 K):  $\delta$  = 6.59 (d,  $J$  = 5.9 Hz, 1H; ArH), 6.50 (d,  $J$  = 6.3 Hz, 1H; ArH), 6.19 (d,  $J$  = 5.9 Hz, 1H; ArH overlapping with m, 8H;  $\text{C}_4\text{H}_2\text{N}$ ), 5.65 (d,  $J$  = 6.34 Hz, 1H; ArH), 4.86 (m, 1H;  $\text{CH}_2$ ), 4.50 (m, 1H;  $\text{CH}_2$ ), 4.32 (m, 1H;  $\text{CH}_2$ ), 3.02 (m, 1H;  $\text{CH}_2$ ), 2.80–1.95 (m, 13H;  $\text{CH}_2$  +  $\text{CHMe}_2$  overlapping with s, 3H;  $\text{CH}_3$ ), 1.40–1.20 (m, 18H;  $\text{CH}_2$ ), 1.23 (t,  $J$  = 7.3 Hz, 3H;  $\text{CH}_3$ ), 1.02 (t,  $J$  = 7.3 Hz, 3H;  $\text{CH}_3$ ), 0.74 (t,  $J$  = 7.3 Hz, 3H;  $\text{CH}_3$ ), 0.57 (t,  $J$  = 7.3 Hz, 3H;  $\text{CH}_3$ ); **3**:  $\text{C}_{46}\text{H}_{62}\text{N}_4\text{NiRu}$ ; calcd C 66.5, H 7.52, N 6.74; found C 66.23, H 7.27, N 6.91.

**Synthesis of 5:**  $[\{\text{Ru}(\text{Cl})(\text{cod})_2(\mu\text{-Cl})_2\}]$  (2.3 g, 4.10 mmol) was refluxed with **1** (7.37 g, 8.20 mmol) in benzene (200 mL) for 12 h. The undissolved LiCl was filtered off and the resulting red solution was evaporated to dryness. The solid residue was triturated with *n*-hexane to give a red powder which was collected and dried in vacuo (3.69 g, 56%). Crystals suitable for X-ray diffraction were grown in a mixture of benzene/*n*-hexane. <sup>1</sup>H NMR ( $\text{C}_6\text{D}_6$ , 200 MHz, 298 K):  $\delta$  = 6.53 (m, 4H;  $\text{C}_4\text{H}_2\text{N}$ ), 6.44 (d,  $J$  = 3.2 Hz, 1H;  $\text{C}_4\text{H}_2\text{N}$ ), 6.38 (d,  $J$  = 3.2 Hz, 1H;  $\text{C}_4\text{H}_2\text{N}$ ), 5.4–5.3 (m, 3H; ArH), 5.05 (s br., 1H;  $\text{C}_4\text{H}_3\text{N}$ ), 4.75 (m, 1H;  $\text{CH}_2$ ), 4.42 (m, 1H;  $\text{CH}_2$ ), 4.23 (m, 1H;  $\text{CH}_2$ ), 3.14 (m, 3H;  $\text{CH}_2$  +  $\text{C}_4\text{H}_3\text{N}$ ), 2.43 (m, 3H;  $\text{CH}_2$  +  $\text{C}_4\text{H}_3\text{N}$ ), 2.1–1.9 (m, 8H;  $\text{CH}_2$ ), 1.85 (m, 1H;  $\text{CH}_2$ ), 1.76 (m, 2H;  $\text{CH}_2$ ), 1.70–1.50 (m, 6H;  $\text{CH}_2$ ), 1.11 (t,  $J$  = 7.3 Hz, 3H;  $\text{CH}_3$ ), 1.03 (t,  $J$  = 7.3 Hz, 3H;  $\text{CH}_3$ ), 0.86 (t,  $J$  = 7.3 Hz, 3H;  $\text{CH}_3$ ), 1.8–1.50 (m, 15H;  $\text{CH}_3$ ); **5**:  $\text{C}_{44}\text{H}_{60}\text{N}_4\text{NiRu}$ ; calcd C 65.67, H 7.51, N 6.96; found C 65.45, H 7.22, N 6.71.

**Synthesis of 6:**  $[\text{CoCl}_2 \cdot \text{THF}_{1.5}]$  (1.31 g, 5.52 mmol) was added in one portion to a solution of **1** (4.96 g, 5.52 mmol) in benzene (100 mL). The reaction mixture, which immediately turned green, was stirred overnight at room temperature. The undissolved solid was filtered off and the solution was evaporated to dryness. The solid residue was triturated with *n*-hexane to give a green solid which was collected and dried in vacuo (3.13 g, 73%). Crystals suitable for X-ray diffraction were grown in DME. They contain benzene of crystallization and  $[\text{Li}(\text{dme})_3]^+$  instead of  $[\text{Li}(\text{thf})_2]^+$  as counteranions. **6**:  $\text{C}_{88}\text{H}_{128}\text{CoLi}_2\text{N}_8\text{Ni}_2\text{O}_4$ ; calcd C 68.09, H 8.31, N 7.21; found C 67.73, H 7.91, N 7.27;  $\mu_{\text{eff}}$  = 1.80  $\mu_{\text{B}}$  at 293 K.

**Photochemical decomposition of 6:** A green solution of **6** (2.0 g, 1.29 mmol) in benzene (300 mL) was exposed to sunlight for several hours until a metallic mirror was formed. The red solution was filtered and analyzed by NMR spectroscopy. The <sup>1</sup>H NMR showed that a mixture of  $[\text{Et}_3\text{N}_4\text{Li}_2\text{Ni}(\text{thf})_4]$  (**1**)<sup>[6]</sup> and  $[\text{Et}_3\text{N}_4\text{Ni}(\Delta)]$  (**7**)<sup>[3a]</sup> was formed. <sup>1</sup>H NMR ( $\text{C}_6\text{D}_6$ , 400 MHz, 298 K):  $\delta$  = 6.61 (d,  $J$  = 5.2 Hz, 2H;  $\text{C}_4\text{H}_2\text{N}$ , **7**), 6.57 (d,  $J$  = 2.8 Hz, 2H;  $\text{C}_4\text{H}_2\text{N}$ , **7**), 6.35 (d,  $J$  = 2.8 Hz, 2H;  $\text{C}_4\text{H}_2\text{N}$ , **7**), 6.17 (s, 8H;  $\text{C}_4\text{H}_2\text{N}$ , **1**), 6.13 (d,  $J$  = 5.2 Hz, 2H;  $\text{C}_4\text{H}_2\text{N}$ , **7**), 3.54 (q,  $J$  = 7.2 Hz, 2H;  $\text{CH}_2$ , **7**), 3.23 (m, 16H; THF, overlapping with m, 8H;  $\text{CH}_2$ , **1**), 2.80 (q,  $J$  = 7.2 Hz, 2H;  $\text{CH}_2$ , **7**), 2.53 (q,  $J$  = 7.2 Hz, 2H;  $\text{CH}_2$ , **7**), 2.28 (q,  $J$  = 7.32 Hz, 8H;  $\text{CH}_2$ , **1** overlapping with m, 2H;  $\text{CH}_2$ , **7**), 1.81 (m, 4H;  $\text{CH}_2$ , **7**), 1.62 (dq,  $J_{\text{gem}}$  = 14.4 Hz,  $J_{\text{vic}}$  = 7.2 Hz, 2H;  $\text{CH}_2$ , **7**), 1.46 (t,  $J$  = 7.2 Hz, 3H;  $\text{CH}_3$ , **7**), 1.42 (t,  $J$  = 7.2 Hz, 3H;  $\text{CH}_3$ , **7**), 1.25 (m, 16H; THF, overlapping with m, 12H;  $\text{CH}_3$ , **1** and m, 2H;  $\text{CH}_2$ , **7**), 1.02 (m, 18H;  $\text{CH}_3$ , **1** + **7**), 0.70 (t,  $J$  = 7.2 Hz, 6H;

CH<sub>3</sub>, **7**), 0.65 (t,  $J = 7.2$  Hz, 3H; CH<sub>3</sub>, **7**), 0.42 (t,  $J = 7.2$  Hz, 3H; CH<sub>3</sub>, **7**). The solution was then concentrated until a crystalline solid precipitated. The product was collected and dried in vacuo (0.32 g, 42%). The <sup>1</sup>H NMR showed that this product was the oxidized form of *meso*-octaethylporphyrinogen containing a mono-cyclopropane unit, **7**.<sup>[3a]</sup> <sup>1</sup>H NMR (C<sub>6</sub>D<sub>6</sub>, 400 MHz, 298 K):  $\delta = 6.61$  (d,  $J = 5.2$  Hz, 2H; C<sub>4</sub>H<sub>2</sub>N), 6.57 (d,  $J = 2.8$  Hz, 2H; C<sub>4</sub>H<sub>2</sub>N), 6.35 (d,  $J = 2.8$  Hz, 2H; C<sub>4</sub>H<sub>2</sub>N), 5.13 (d,  $J = 5.2$  Hz, 2H; C<sub>4</sub>H<sub>2</sub>N), 3.54 (q,  $J = 7.2$  Hz, 2H; CH<sub>2</sub>), 2.80 (q,  $J = 7.2$  Hz, 2H; CH<sub>2</sub>), 2.53 (q,  $J = 7.2$  Hz, 2H; CH<sub>2</sub>), 2.27 (dq,  $J_{gem} = 14.4$  Hz,  $J_{vic} = 7.2$  Hz, 2H; CH<sub>2</sub>), 1.81 (m, 4H; CH<sub>2</sub>), 1.62 (dq,  $J_{gem} = 14.4$  Hz,  $J_{vic} = 7.2$  Hz, 2H; CH<sub>2</sub>), 1.46 (t,  $J = 7.2$  Hz, 3H; CH<sub>3</sub>), 1.42 (t,  $J = 7.2$  Hz, 3H; CH<sub>3</sub>), 1.20 (q,  $J = 7.2$  Hz, 2H; CH<sub>2</sub>), 1.02 (t,  $J = 7.2$  Hz, 6H; CH<sub>3</sub>), 0.70 (t,  $J = 7.2$  Hz, 6H; CH<sub>3</sub>), 0.65 (t,  $J = 7.2$  Hz, 3H; CH<sub>3</sub>), 0.42 (t,  $J = 7.2$  Hz, 3H; CH<sub>3</sub>).

**Synthesis of 8:** [NiCl<sub>2</sub> · DME] (3.67 g, 16.7 mmol) was added in one portion to a solution of **1** (15 g, 16.7 mmol) in THF (400 mL). The reaction mixture, which immediately turned violet, was stirred overnight at room temperature. The solvent was evaporated and benzene (500 mL) was added. The undissolved LiCl was filtered off and the solution was evaporated to dryness. The solid residue was triturated with *n*-hexane to give a microcrystalline blue-violet solid, which was collected and dried in vacuo (9.11 g, 79%). Crystals suitable for X-ray diffraction were grown in a mixture of DME/dioxane. They contain DME and dioxane of crystallization, along with [Li(dme)<sub>3</sub>]<sup>+</sup> as counteranion. **8**: C<sub>80</sub>H<sub>112</sub>ClLiNi<sub>8</sub>N<sub>4</sub>O<sub>2</sub>; calcd C 64.27, H 7.55, N 7.49; found C 64.33, H 7.52, N 7.57;  $\mu_{eff} = 2.85 \mu_B$  at 293 K per nickel.

**Thermal decomposition of 8, synthesis of 9 + 10:** A blue-violet solution of **8** (1.52 g, 1.10 mmol) in benzene (100 mL) was refluxed overnight. The reaction mixture turned red and a metallic mirror was formed. The solution was filtered and analyzed by NMR spectroscopy. The <sup>1</sup>H NMR of the solution showed that an equimolar mixture of [(Et<sub>6</sub>N<sub>4</sub>)Ni] (**9**), and the two dihydro-2,12 and -2,13 isomers [Et<sub>6</sub>H<sub>2</sub>N<sub>4</sub>)Ni] **10a** and **10b**<sup>[7]</sup> were formed. <sup>1</sup>H NMR (C<sub>6</sub>D<sub>6</sub>, 400 MHz, 298 K):  $\delta = 7.08$  (d,  $J = 4.0$  Hz, 4H; C<sub>4</sub>H<sub>2</sub>N, **9**), 6.35 (d,  $J = 3.2$  Hz, 2H; C<sub>4</sub>H<sub>2</sub>N, **10a**), 6.31 (d, 4H;  $J = 4.0$  Hz, C<sub>4</sub>H<sub>2</sub>N, **9** overlapping with s, 2H; C<sub>4</sub>H<sub>2</sub>N, **10b**), 6.23 (s, 2H; C<sub>4</sub>H<sub>2</sub>N, **10b**), 6.16 (d,  $J = 3.2$  Hz, 2H; C<sub>4</sub>H<sub>2</sub>N, **10a**), 5.33 (t,  $J = 2.4$  Hz, 2H; C<sub>4</sub>H<sub>2</sub>N, **10a**), 5.31 (t,  $J = 2.0$  Hz, 2H; C<sub>4</sub>H<sub>2</sub>N, **10b**), 3.83 (dq,  $J_{gem} = 13.8$  Hz,  $J_{vic} = 7.2$  Hz, 4H; CH<sub>2</sub>), 3.54 (dq,  $J_{gem} = 13.6$  Hz,  $J_{vic} = 7.2$  Hz, 2H; CH<sub>2</sub>), 3.43 (m, 6H; CH<sub>2</sub>, **9 + 10**), 3.24 (dq,  $J_{gem} = 13.6$  Hz,  $J_{vic} = 7.2$  Hz, 2H; CH<sub>2</sub>), 3.04 (dq,  $J_{gem} = 13.2$  Hz,  $J_{vic} = 7.6$  Hz, 2H; CH<sub>2</sub>), 2.80–2.70 (m, 4H; CH<sub>2</sub> overlapping with d,  $J = 2.0$  Hz, 4H; C<sub>4</sub>H<sub>2</sub>N, d,  $J = 2.0$  Hz, 2H; C<sub>4</sub>H<sub>2</sub>N, d,  $J = 2.0$  Hz, 2H; C<sub>4</sub>H<sub>2</sub>N), 2.60 (q,  $J = 7.8$  Hz, 4H; CH<sub>2</sub>, **9**), 2.44 (dq,  $J_{gem} = 13.6$  Hz,  $J_{vic} = 7.2$  Hz, 2H; CH<sub>2</sub>), 2.1–2.0 (m, 8H; CH<sub>2</sub>), 1.97 (m, 8H; CH<sub>2</sub>, **9 + 10**), 1.67 (dq,  $J_{gem} = 14.4$  Hz,  $J_{vic} = 7.2$  Hz, 2H; CH<sub>2</sub>), 1.57 (dq,  $J_{gem} = 14.4$  Hz,  $J_{vic} = 7.2$  Hz, 2H; CH<sub>2</sub>), 1.22 (t,  $J = 7.2$  Hz, 6H; CH<sub>3</sub>), 1.19 (t,  $J = 7.6$  Hz, 6H; CH<sub>3</sub>), 1.1–0.90 (m, 36H; CH<sub>3</sub>, **9 + 10**), 0.86 (t,  $J = 7.2$  Hz, 6H; CH<sub>3</sub>), 0.81 (t,  $J = 7.2$  Hz, 6H; CH<sub>3</sub>), 0.73 (t,  $J = 7.2$  Hz, 6H; CH<sub>3</sub>).

**Reaction of 8 with CO:** A blue-violet solution of **8** (2.3 g, 1.66 mmol) in benzene (200 mL) was maintained under an atmosphere of CO overnight. The reaction mixture turned red and a solid precipitated. Analysis by <sup>1</sup>H NMR spectroscopy of the solution showed only the [Et<sub>6</sub>N<sub>4</sub>Ni(Δ)] (**7**),<sup>[1b,3]</sup> while [Ni(CO)<sub>4</sub>] was detected by IR spectroscopy ((C<sub>6</sub>H<sub>6</sub>,  $\nu_{max}$  [cm<sup>-1</sup>]) 2040(s)). The suspension was filtered and the solid residue was treated with benzene to dissolve the product coprecipitated with LiCl. The solution was then evaporated to dryness and the solid residue was triturated with *n*-hexane (50 mL) to give a red powder which was collected and dried in vacuo (1.6 g, 81%). <sup>1</sup>H NMR (C<sub>6</sub>D<sub>6</sub>, 400 MHz, 298 K):  $\delta = 6.61$  (d,  $J = 5.2$  Hz, 2H; C<sub>4</sub>H<sub>2</sub>N), 6.57 (d,  $J = 2.8$  Hz, 2H; C<sub>4</sub>H<sub>2</sub>N), 6.35 (d,  $J = 2.8$  Hz, 2H; C<sub>4</sub>H<sub>2</sub>N), 5.13 (d,  $J = 5.2$  Hz, 2H; C<sub>4</sub>H<sub>2</sub>N), 3.54 (q,  $J = 7.2$  Hz, 2H; CH<sub>2</sub>), 2.80 (q,  $J = 7.2$  Hz, 2H; CH<sub>2</sub>), 2.53 (q,  $J = 7.2$  Hz, 2H; CH<sub>2</sub>), 2.27 (dq,  $J_{gem} = 14.4$  Hz,  $J_{vic} = 7.2$  Hz, 2H; CH<sub>2</sub>), 1.81 (m, 4H; CH<sub>2</sub>), 1.62 (dq,  $J_{gem} = 14.4$  Hz,  $J_{vic} = 7.2$  Hz, 2H; CH<sub>2</sub>), 1.46 (t,  $J = 7.2$  Hz, 3H; CH<sub>3</sub>), 1.42 (t,  $J = 7.2$  Hz, 3H; CH<sub>3</sub>), 1.20 (q,  $J = 7.2$  Hz, 2H; CH<sub>2</sub>), 1.02 (t,  $J = 7.2$  Hz, 6H; CH<sub>3</sub>), 0.70 (t,  $J = 7.2$  Hz, 6H; CH<sub>3</sub>), 0.65 (t,  $J = 7.2$  Hz, 3H; CH<sub>3</sub>), 0.42 (t,  $J = 7.2$  Hz, 3H; CH<sub>3</sub>).

**X-ray crystallography for complexes 2, 3, 5, 6, and 8:** Crystals of **2**, **3**, **5**, **6**, and **8** were mounted in glass capillaries and sealed under nitrogen. Diffraction data for complex **2**, **3**, and **5** were collected on a Rigaku AFC6S four-circle diffractometer at 296 K (**2**) and 143 K (**3**, **5**) and reduced with teXsan for Windows release 1.0.1.<sup>[21]</sup> Data for complex **6** were collected on a KUMA CCD at 143 K and reduced with KM4RED release 1.5.2.<sup>[22]</sup> Data for complex **8** were collected on a mar345 Image Plate Detector at 143 K and reduced with marHKL release 1.9.1.<sup>[23]</sup> No absorption correction was

applied to any data set. Structure solution for compounds **2**, **3**, **5**, and **8** was performed with ab-initio direct methods,<sup>[24]</sup> whereas for compound **6** the heavy atom Patterson methods<sup>[25]</sup> were applied. All structures were refined by using the full-matrix least-squares on  $F^2$  with all non-H atoms anisotropically refined, except **5** for which a low ratio obs/par allowed us to refine the two metals and the nitrogens in an anisotropic manner. Hydrogen atoms were placed in calculated positions using the riding model with  $U_{iso} = a * U_{eq}(X)$  (where  $a$  is 1.5 for methyl hydrogen atoms and 1.2 for others, while  $X$  is the parent atom), in some cases for methyl hydrogen atoms and for hydrogen atoms belonging to solvent molecules a common isotropic displacement parameter ( $U_{iso} = 0.08 \text{ \AA}^2$ ) was used. In the last stage of refinement the weighting adopted scheme [ $1/(w^2(F_o^2) + (aP)^2 + bP)$ , where  $P = (F_o^2 + 2F_c^2)/3$ ] gave the following result for  $a$  and  $b$ , respectively (0.0605, 81.7582, **2**; 0.0512, 9.0460, **3**; 0.0439, 16.8658, **5**; 0.0888, 15.0068, **6**; 0.1515, 4.5857, **8**). Due to the presence of disorder some restraints/constraints were applied to two structures. In complex **6**, the benzene ring was fitted to a regular hexagon. In complex **8**, geometrical and rigid body restraints were applied to two ethyl chains. Structure solution, refinement, molecular graphics, and geometrical calculation were carried out on all structures with the SHELXTL software package, release 5.1.<sup>[26]</sup> Crystallographic data (excluding structure factors) for the structures reported in this paper have been deposited with the Cambridge Crystallographic Data Centre as supplementary publication nos. CCDC-116222 for **2**, CCDC-116223 for **3**, CCDC-116224 for **5**, CCDC-116225 for **6**, CCDC-116226 for **8**. Copies of the data can be obtained free of charge on application to CCDC, 12 Union Road, Cambridge CB2 1EZ, UK (fax: (+44) 1223-336-033; e-mail: deposit@ccdc.cam.ac.uk).

## Acknowledgments

We thank the Fonds National Suisse de la Recherche Scientifique (Bern, Switzerland, Grant No. 20-53336.98), Ciba Specialty Chemicals (Basle, Switzerland), and Action COST D9 (European Program for Scientific Research, OFES No. C98.008) for financial support.

- [1] General references are made to: a) C. Floriani, *Pure Appl. Chem.* **1996**, *68*, 1–8; b) C. Floriani, *Chem. Commun.* **1996**, 1257–1263.
- [2] a) D. Jacoby, S. Isoz, C. Floriani, A. Chiesi-Villa, C. Rizzoli, *J. Am. Chem. Soc.* **1995**, *117*, 2793–2804; b) D. Jacoby, S. Isoz, C. Floriani, A. Chiesi-Villa, C. Rizzoli, *J. Am. Chem. Soc.* **1995**, *117*, 2805–2816; c) C. Floriani, in *Stereoselective Reactions of Metal-Activated Molecules* (Eds.: H. Werner, J. Sundermeyer), Vieweg, Wiesbaden, **1995**, pp. 97–106; d) S. De Angelis, E. Solari, C. Floriani, A. Chiesi-Villa, C. Rizzoli, *Organometallics* **1995**, *14*, 4505–4512; e) D. Jacoby, S. Isoz, C. Floriani, K. Schenk, A. Chiesi-Villa, C. Rizzoli, *Organometallics* **1995**, *14*, 4816–4824; f) S. Isoz, C. Floriani, K. Schenk, A. Chiesi-Villa, C. Rizzoli, *Organometallics* **1996**, *15*, 337–344.
- [3] a) S. De Angelis, E. Solari, C. Floriani, A. Chiesi-Villa, C. Rizzoli, *J. Am. Chem. Soc.* **1994**, *116*, 5691–5701; b) S. De Angelis, E. Solari, C. Floriani, A. Chiesi-Villa, C. Rizzoli, *J. Am. Chem. Soc.* **1994**, *116*, 5702–5713; c) U. Piarulli, E. Solari, C. Floriani, A. Chiesi-Villa, C. Rizzoli, *J. Am. Chem. Soc.* **1996**, *118*, 3634–3642.
- [4] a) S. De Angelis, E. Solari, C. Floriani, A. Chiesi-Villa, C. Rizzoli, *Angew. Chem.* **1995**, *107*, 1200–1202; *Angew. Chem. Int. Ed. Engl.* **1995**, *34*, 1092–1094; b) C. Floriani, E. Solari, G. Solari, A. Chiesi-Villa, C. Rizzoli, *Angew. Chem.* **1998**, *110*, 2367–2369; *Angew. Chem. Int. Ed.* **1998**, *37*, 2245–2248, and references therein.
- [5] For the relevance of the  $\pi$ -bonding ability of the polypyrrole structure see: M. O. Senge, *Angew. Chem.* **1996**, *108*, 2051–2053; *Angew. Chem. Int. Ed. Engl.* **1996**, *35*, 1923–1925, and references therein.
- [6] J. Jubb, D. Jacoby, C. Floriani, A. Chiesi-Villa, C. Rizzoli, *Inorg. Chem.* **1992**, *31*, 1306–1308.
- [7] L. Bonomo, E. Solari, C. Floriani, A. Chiesi-Villa, C. Rizzoli, *J. Am. Chem. Soc.* **1998**, *120*, 12972–12973.
- [8] C. S. Alexander, S. J. Rettig, B. R. James, *Organometallics* **1994**, *13*, 2542–2544.
- [9] For  $\pi$  binding between aromatic metalla-porphyrins and a metal see: K. Koczaja Dailey, G. P. A. Yap, A. L. Rheingold, T. B. Rauchfuss,

- Angew. Chem.* **1996**, *108*, 1985–1987; *Angew. Chem. Int. Ed. Engl.* **1996**, *35*, 1833–1835.
- [10] M. A. Bennett, A. K. Smith, *J. Chem. Soc. Dalton Trans.* **1974**, 233–241.
- [11] a) E. W. Abel, M. A. Bennett, G. Wilkinson, *J. Chem. Soc.* **1959**, 3178–3182; b) J. Powell, B. L. Shaw, *J. Chem. Soc. (A)* **1968**, 159–161; c) J. Müller, C. G. Kreiter, B. Mertshenk, S. Schmitt, *Chem. Ber.* **1975**, *108*, 273–282; d) S. D. Robinson, G. Wilkinson, *J. Chem. Soc. (A)* **1966**, 300–301; e) T. A. Stephenson, E. S. Switkes, L. Ruiz-Ramirez, *J. Chem. Soc. Dalton Trans.* **1973**, 2112–2114.
- [12] F. Kvietok, V. Allured, V. Carperos, M. Rakowski Dubois, *Organometallics* **1994**, *13*, 60–68.
- [13] E. A. Seddon, K. R. Seddon, *The Chemistry of Ruthenium* (Ed.: R. J. Clark), Elsevier, Amsterdam, **1984**.
- [14] *Comprehensive Coordination Chemistry II, Vol. 7* (Eds.: E. W. Abel, F. G. A. Stone, G. Wilkinson), Pergamon, Oxford, **1995**, Ch. 7, 8, 9, 10.
- [15] F. B. McCormick, D. D. Cox, W. B. Gleason, *Organometallics* **1993**, *12*, 610–612, and references therein.
- [16] D. L. Kershner, A. L. Rheingold, F. Basolo, *Organometallics* **1987**, *6*, 196–198.
- [17] H. Wadepohl, W. Galm, H. Pritzkov, A. Wolf, *Chem. Eur. J.* **1996**, *2*, 1453–1465.
- [18] L. Bonomo, E. Solari, C. Floriani, unpublished results.
- [19] a) A. G. Lappin, *Redox Mechanisms in Inorganic Chemistry*, Ellis Horwood, Chichester, U. K., **1994**; b) *Electron Transfer in Biology and the Solid State* (Eds.: M. K. Johnson, R. B. King, D. M. Kurtz Jr., C. Kutal, M. L. Norton, R. A. Scott), ACS, Washington DC, **1990**.
- [20] a) R. Taube, S. Wache, J. Sieler, R. Kempe, *J. Organomet. Chem.* **1993**, *456*, 131–136; b) J. Sieler, R. Kempe, S. Wache, R. Taube, *J. Organomet. Chem.* **1993**, *455*, 241–246; c) H. Lehmkuhl, J. Näser, G. Mehler, T. Keil, F. Danowski, R. Benn, R. Mynott, G. Schroth, B. Gabor, C. Krüger, P. Betz, *Chem. Ber.* **1991**, *124*, 441–452.
- [21] Molecular Structure Corporation, a Rigaku company, 3200 Research Forest Drive The Woodlands, TX 77381–4238, USA, **1997**.
- [22] Kuma Diffraction Instruments GmbH, PSE-EPFL module 3.4, CH-1015, Lausanne, Switzerland, **1999**.
- [23] Z. Otwinowski, W. Minor, *Methods in Enzymology, Vol. 276: Macromolecular Crystallography* (Eds.: C. W. Carter, Jr., R. M. Sweet), Academic Press, **1997**, part A, pp. 307–326.
- [24] G. M. Sheldrick, *Acta Crystallogr. Sect. A* **1990**, *46*, 467–473.
- [25] G. M. Sheldrick, Z. Dauter, K. S. Wilson, H. Hope, L. C. Sieker, *Acta Crystallogr. Sect. D* **1993**, *49*, 18–23.
- [26] Bruker AXS, Inc., Madison, Wisconsin, 53719, USA, **1997**.

Received: March 15, 1999 [F1677]